FULL PAPER

Organic Photovoltaics

ADVANCED
FUNCTIONAL
MATERIALS
www.afm-journal.de

Random Copolymers Outperform Gradient and Block Copolymers in Stabilizing Organic Photovoltaics

Chen Kong, Byeongseop Song, Emily A. Mueller, Jinsang Kim, and Anne J. McNeil*

Recent advances have led to conjugated polymer-based photovoltaic devices with efficiencies rivaling amorphous silicon. Nevertheless, these devices become less efficient over time due to changes in active layer morphology, thereby hindering their commercialization. Copolymer additives are a promising approach toward stabilizing blend morphologies; however, little is known about the impact of copolymer sequence, composition, and concentration. Herein, the impact of these parameters is determined by synthesizing random, block, and gradient copolymers with a poly(3-hexylthiophene) (P3HT) backbone and side-chain fullerenes (phenyl-C_{61}-butyric acid methyl ester ($PC_{61}BM$)). These copolymers are evaluated as compatibilizers in photovoltaic devices with $P3HT:PC_{61}BM$ as the active layer. The random copolymer with 20 mol% fullerene side chains and at 8 wt% concentration in the blend gives the most stable morphologies. Devices containing the random copolymer also exhibit higher and more stable power conversion efficiencies than the control device. Combined, these studies point to the random copolymer as a promising new scaffold for stabilizing bulk heterojunction photovoltaics.

1. Introduction

The National Renewable Energy Lab (NREL) has been tracking the "best" photovoltaic cells since 1976, highlighting growth trends in promising materials and technologies.[1] Conjugated polymer-based solar cells exhibit some of the lowest efficiencies on this chart but are considered "emerging" materials because of their advantageous properties, including transparency,

Dr. C. Kong, E. A. Mueller, Prof. A. J. McNeil
Department of Chemistry and Macromolecular Science
and Engineering Program
University of Michigan
930 North University Avenue, Ann Arbor, MI 48109-1055, USA
E-mail: ajmcneil@umich.edu
Dr. B. Song
Department of Electrical Engineering and Computer Science
University of Michigan
Ann Arbor, MI 48109, USA
Prof. J. Kim
Department of Materials Science and Engineering
Department of Macromolecular Science and Engineering
Department of Chemistry
Department of Chemical Engineering
University of Michigan
Ann Arbor, MI 48109, USA

The ORCID identification number(s) for the author(s) of this article can be found under https://doi.org/10.1002/adfm.201900467.

DOI: 10.1002/adfm.201900467

flexibility, and low weight.[2] In addition, the solution-based processing methods used for device fabrication are commercially appealing.[3] As a consequence, many researchers continue searching for organic materials with higher efficiencies.

Most organic photovoltaics are constructed from a blend of two materials: a conjugated polymer electron donor and a small molecule electron acceptor. The optoelectronic properties and device performance are dictated by the chemical structures of both components as well as the blend morphology. Recent advances in both donor and acceptor structures have led to organic devices with efficiencies that rival amorphous silicon.[2a,4,5] As an example, Hou et al. described a novel blend with a record-breaking 14.2% efficiency.[4a] This device has not yet been certified by NREL due to its instability. In a corresponding highlight article, Hou suggests that conjugated polymer-based devices may reach 18–20% efficiency within the next few years.[6]

With efficiencies on the rise, many researchers are focusing on improving device longevity. Due to changes in the active layer morphology, organic photovoltaic devices gradually lose efficiency over time.[7] The initial active layer morphology consists of nanoscale phase-separated poly(3-hexylthiophene) (P3HT) and phenyl-C_{61}-butyric acid methyl ester ($PC_{61}BM$) domains. These domains coalesce, increasing in size over time due to enthalpically driven phase separation.[8] The net result is that the power conversion efficiencies (PCE) dramatically decrease, reducing the device utility.

To attenuate this detrimental process, researchers are investigating compatibilizers—a third component added to the blend to stabilize the morphology through noncovalent interactions.[9] To be effective, the compatibilizer should minimize the overall free energy by localizing at the donor/acceptor interface, lowering the interfacial tension, and suppressing domain coalescence. The compatibilizer can impart additional beneficial properties to the device, such as a broader and stronger absorption profile as well as more efficient exciton dissociation and charge transport, all of which would contribute to a higher PCE.[9]

Both small molecules[10] and polymers[11,12] have been used as compatibilizers with moderate success. The majority of polymer compatibilizers have been diblock copolymers containing repeat units that are structurally similar to the donor and acceptor.[12] A prototypical example is a rod–coil diblock copolymer with a conjugated segment (the rod) that resembles

**ADVANCED
SCIENCE NEWS**
www.advancedsciencenews.com

**ADVANCED
FUNCTIONAL
MATERIALS**
www.afm-journal.de

the donor polymer and a nonconjugated segment (the coil) with a side-chain group that interacts with the acceptor. One limitation of this approach is that the coil segment is frequently an insulating material, which lowers the effective concentration of absorbing and electroactive species in the device. Rod–rod diblock copolymers wherein both segments are conjugated have also been used.[12] These copolymers can facilitate exciton dissociation and charge transport as well. Although adding these tailored compatibilizers provides longer-lasting devices, no studies have elucidated the impact of sequence (e.g., block vs gradient) or composition (e.g., 50:50 vs 25:75) on compatibilization.

To address this knowledge gap, we have been exploring alternative copolymer sequences (i.e., random[13] and gradient[14,15] copolymers) as compatibilizers in blends. For example, we reported that gradient copolymer compatibilizers led to smaller domain sizes than the analogous block and random copolymers in homopolymer blends.[14] Gradient copolymers, with their gradual compositional change, were best at interacting with both homopolymer domains to lower the interfacial energy. In related work, we found that a gradient copolymer could stabilize photovoltaic devices containing P3HT and $PC_{61}BM$, with little change in efficiency over extended thermal annealing times (>60 min at 150 °C).[15]

Herein, we expand on this work by examining the influence of copolymer sequence (random, diblock, and gradient), composition (comonomer ratio), and concentration on the stabilization of $P3HT:PC_{61}BM$ blends. All copolymers attenuated phase separation during thermal annealing. Their compatibilizing abilities depended on copolymer sequence, with gradient and random sequences outperforming the analogous diblock sequences. Further studies showed that the random copolymer gave a higher and longer-lasting PCE than the blend without copolymer. These improvements were due to the random copolymer's ability to stabilize the morphology, as well as facilitate exciton dissociation and charge transport. Combined, these results suggest that random copolymers are the best compatibilizers for stabilizing organic photovoltaics.

2. Results and Discussion

2.1. Synthesis and Characterization of Copolymer Additives

Nine copolymers were targeted each with a different sequence and/or composition. The copolymers had a poly(3-hexylthiophene) backbone with varying quantities and distributions of side-chain fullerenes. Catalyst-transfer polymerization (CTP)[16] was used to access all copolymers with random, gradient, and block sequences, narrow dispersities (Đ), and high regioregularities (**Scheme 1**). Polymers with approximately the same number-average molecular weights (M_n) were targeted by using the same monomer/catalyst ratio for each polymerization. Using a precatalyst with an *ortho*-tolyl reactive ligand[15,17,18] ensured unidirectional propagation and led to polymers with tolyl/H end groups. Activated (5-bromo-4-hexylthiophen-2-yl) magnesium chloride (HT) and (5-bromo-4-(6-bromohexyl)thiophen-2-yl)magnesium chloride (BrHT) were chosen as monomers to generate polymers with specified reactive side-chain distributions. Using this approach, we synthesized random,
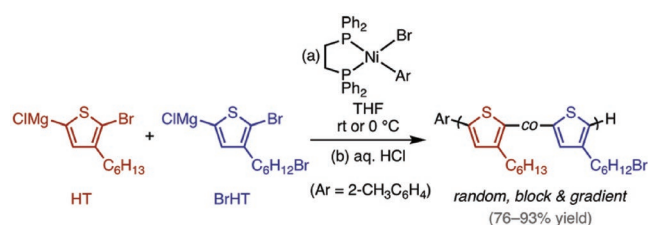

Scheme 1. Copolymer synthesis with random, block, and gradient distributions of Br-functionalized side chains.

gradient, and diblock[19] copolymers with three different theoretical HT:BrHT ratios (80:20, 65:35, and 50:50; pp. S24–S44, Supporting Information).[15]

The gradient copolymers were prepared by initiating HT polymerization and then gradually adding BrHT. The block copolymers were prepared by adding precatalyst to a solution containing HT; once the HT consumption reached >90%, BrHT was added. The random copolymers were prepared by adding precatalyst to a solution containing both HT and BrHT. A random (rather than statistical) sequence was obtained due to the similar monomer reactivities.[14e] The cumulative mole fraction incorporation of BrHT (f_{BrHT}) versus the copolymer's normalized chain length was evaluated by running an independent set of polymerizations where aliquots were periodically removed (**Figure 1**). As anticipated, the random copolymer showed a consistent, cumulative HT:BrHT ratio, whereas the block and gradient copolymers showed a changing HT:BrHT ratio consistent with the time-dependent changes in relative monomer concentrations during the reaction.

For each copolymer, a chain length of 80 thiophene units was targeted using a monomer/catalyst ratio of 80/1, which would give theoretical M_n of ≈14–15 kg mol^{-1} depending on the BrHT mole fraction. The experimental M_n ranged from 18 to 22 kg mol^{-1}, consistent with the known overestimation of gel permeation chromatography (GPC) by a factor of ≈1.3× when using polystyrene calibration standards (**Table 1**).[21] As anticipated for CTP, each copolymer sample exhibited low dispersity (Đ = 1.11–1.24) and high regioregularity (pp. S35–S44, Supporting Information). In addition, the mole fraction of BrHT
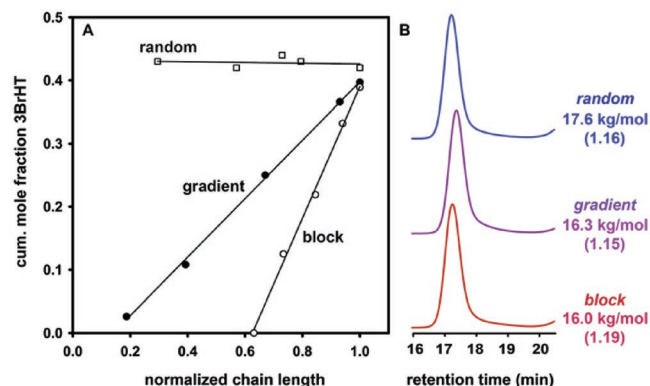

Figure 1. A) Plot of the cumulative BrHT mole fraction in each copolymer versus its normalized chain length with a total monomer feed ratio of 60:40 HT:BrHT.[20] B) GPC traces for the polymers obtained at normalized chain length = 1 (M_n and Đ are shown).

Table 1. Data for copolymers with Br-functionalized side chains.

BrHT:HT [mol:mol]	Block			Random			Gradient		
	50:50	35:65	20:80	50:50	35:65	20:80	50:50	35:65	20:80
M_n [kg mol^{-1}]	18.8	19.1	19.5	21.1	21.4	21.7	20.7	22.1	18.9
Đ	1.19	1.17	1.15	1.24	1.23	1.22	1.15	1.11	1.19
f_{BrHT}	0.52	0.36	0.21	0.51	0.35	0.21	0.53	0.34	0.20

incorporated into the copolymer (f_{BrHT}) matched the experimental feed ratios, implying that their conversion rates were similar.

Two postpolymerization reactions were used to append fullerene units onto the copolymer side chains. The first reaction used sodium azide to substitute the side-chain bromine with an azide, generating a reactive handle for the click reaction (**Scheme 2**).[15,22] Subsequent ^{1}H NMR spectroscopic analysis revealed quantitative conversion of Br to N$_3$. In addition, there were no significant changes in the GPC profiles. The second reaction involved an azide–alkyne "click" reaction to install the fullerene moieties onto the side chain. In our previous work, we used the copper-catalyzed azide–alkyne cycloaddition;[15a] however, crosslinked polymers were obtained when the azide concentration exceeded 10 mol%. To prevent this deleterious side reaction, we employed the strain-promoted azide–alkyne cycloaddition (SPAAC) that proceeds without a copper catalyst.[23] This approach involved five linear steps to synthesize the strained alkyne fullerene derivative, with a 14% overall yield from commercial starting materials (**Scheme 3**, pp. S8–S11, Supporting Information). Although low yielding, most alternative methods for grafting fullerene to P3HT require harsher conditions, including [3 + 2] cycloadditions,[12f,h,24] 1,3-dipolar cycloadditions,[12a,25] and S$_N$2 reactions.[26] In contrast, the Steglich esterification[27] and Diels–Alder cycloaddition[28] represent mild alternatives to SPAAC for grafting fullerenes to P3HT. Our route began with ring expansion of dibenzosuberenone followed by reduction with sodium borohydride.[29] Subsequent dibromination followed by a double elimination with lithium diisopropylamide afforded dibenzocyclooctynol (DIBO) in moderate yield.[29] In a separate step, the
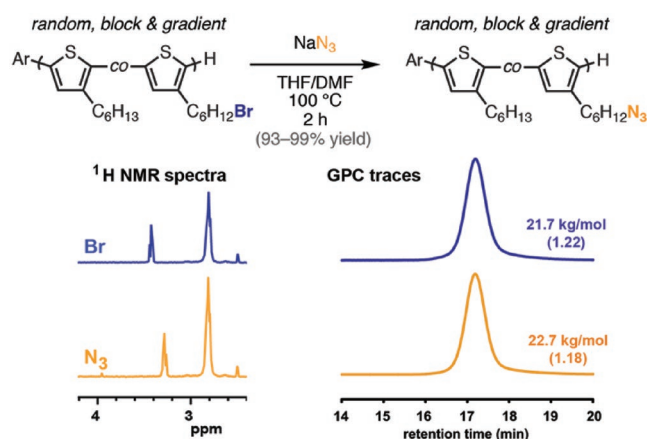
methyl ester of PC$_{61}$BM was converted to the corresponding acid via hydrolysis.[30] Esterifying this acid with DIBO in the presence of N,N'-diisopropylcarbodiimide yielded the click-ready fullerene derivative PC$_{61}$B-DIBO.[15]
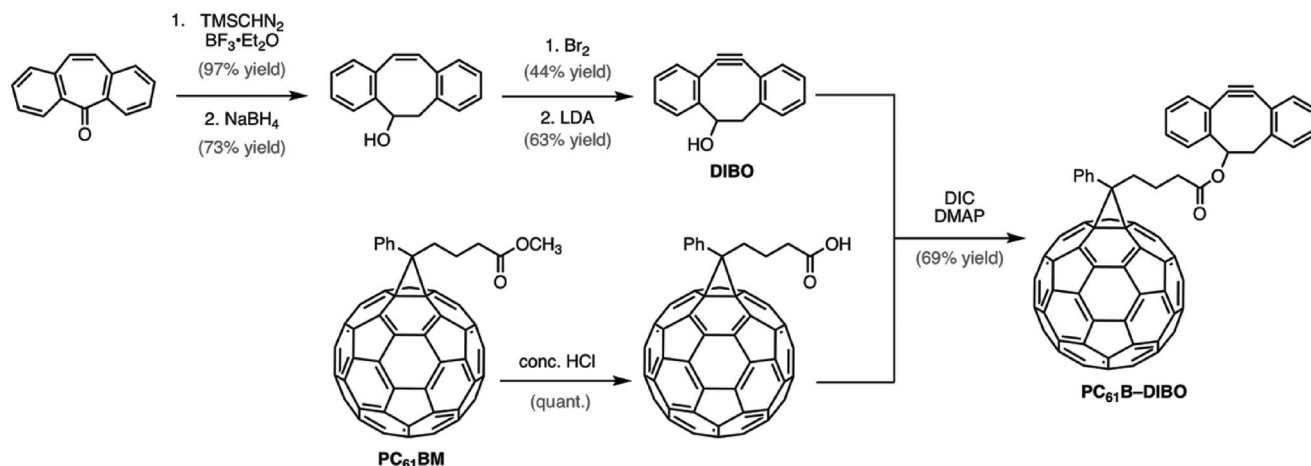
Each of the nine copolymers were functionalized with fullerene via SPAAC by stirring the azide-functionalized copolymer with PC$_{61}$BM-DIBO at room temperature over 48 h (**Scheme 4**, pp. S51–S56, Supporting Information).[31,32] The fullerene-loaded copolymers were characterized using IR spectroscopy to confirm >95% azide conversion via disappearance of the peak at 2091 cm^{-1}.[33] Comparing the copolymers to a fullerene-functionalized small-molecule analog (pp. S22 and S23, Supporting Information) via ^{1}H NMR spectroscopy supported cycloadduct formation. Multiple stereo- and regioisomers were generated due to both the racemic PC$_{61}$B-DIBO and the non-regioselective reaction. Combined, these results indicate that fullerene-functionalized copolymers with varying sequences and compositions were obtained.

2.2. Quantifying Phase Separation in Blends

As noted above, one of the biggest challenges for polymer-based photovoltaics is their unstable active layer morphologies,[7] which form micrometer-scale domains with reduced interfacial area over time. We hypothesized that fullerene-functionalized P3HT copolymers could enthalpically stabilize P3HT:PC$_{61}$BM blends, minimizing their micrometer-scale phase separation. To test this hypothesis, we examined the thermal stability of P3HT:PC$_{61}$BM blends with and without each copolymer additive using optical microscopy.

The benchmark was set by annealing P3HT:PC$_{61}$BM (1:1 wt:wt) blends for 1 h at 150 °C. Subsequent optical microscope images revealed needle-shaped PC$_{61}$BM aggregates[34] (≈5–30 mm length and ≈1 mm width) occupying 11.4% of the film area (**Figure 2**A). Next, blends with different copolymer sequences and compositions were codeposited with P3HT:PC$_{61}$BM at several different concentrations. After thermal annealing, optical microscope images revealed that all copolymer additives led to reduced sizes and densities of PC$_{61}$BM aggregates (Figure 2B–D, Figures S51–S54, Supporting Information).

Plotting these data as a function of the copolymer variables revealed that the random and gradient sequences outperformed the diblock sequence regardless of the composition or concentration (Figure 2E). We suspect that this effect is entropic in origin, wherein the gradient and random copolymers have more low-energy orientations at the interface (than the block) due to their mixed composition. When comparing copolymers of the same sequence and composition but at different concentrations in the blend (e.g., 2 vs 8 wt%), we found that higher copolymer concentrations were better, presumably because more of the interfacial area can be stabilized under these conditions. When comparing copolymers with the same sequences but different compositions (e.g., random 50 vs 20 mol%), the higher fullerene loading exhibited *more* phase separation. In this case, less compatibilizer is added to the blend when the fullerene-loading is higher because the average "repeat unit" mass is higher; consequently, less interfacial area

Scheme 2. Postpolymerization reaction to generate random, block, and gradient copolymers with N$_3$-functionalized side chains. ^{1}H NMR spectra and GPC traces of the random copolymer (20 mol%) before and after the reaction.

ADVANCED
SCIENCE NEWS
www.advancedsciencenews.com

ADVANCED
FUNCTIONAL
MATERIALS
www.afm-journal.de

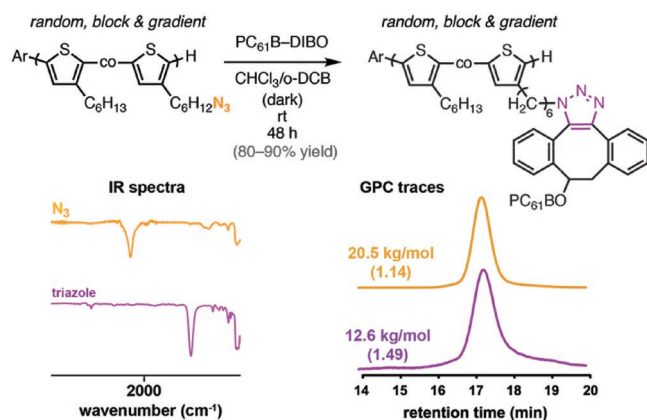**Scheme 3.** Synthetic route to generate PC$_{61}$B-DIBO from dibenzosuberenone and PC$_{61}$BM.

is stabilized under these conditions. In total, these data suggested that the most stable devices would be obtained with random and/or gradient copolymers at 20 mol% fullerene loading and at 8 wt% concentration in the blend.

These conclusions are further supported by UV–vis spectroscopic data collected on selected films before and after thermal annealing (Figure S55, Supporting Information). The blend with no additive showed substantial phase separation after annealing as evidenced by a drop in the PC$_{61}$BM signal (due to crystallization) and an increase in the P3HT peak intensity (due to demixing). In contrast, a blend containing random copolymer (20 mol% fullerene, at 8 wt% concentration) showed no change in the PC$_{61}$BM intensity and only a small increase in P3HT intensity after thermal annealing.

Combined, these results indicate that all copolymers suppress phase separation in P3HT:PC$_{61}$BM blends, presumably by serving as an interfacial compatibilizer. One alternative explanation is that the copolymer increases the glass transition temperature of the blend (T_g^{blend}), which would minimize phase separation at the temperatures studied herein. To evaluate this hypothesis, the T_g^{blend} was measured for blends with and without added copolymer via differential scanning calorimetry (DSC). Blends without the copolymers exhibited a weak, broad T_g^{blend} at 42 °C, consistent with previous reports (Figure S69, Supporting Information).[35] In contrast, blends containing the copolymer additive did not exhibit a discernable T_g^{blend}, regardless of sample mass, scan rate, scan range, and even with a modulated temperature profile (pp. S69–S71, Supporting Information). At this time, the precise mechanism for the stabilization remains unclear.
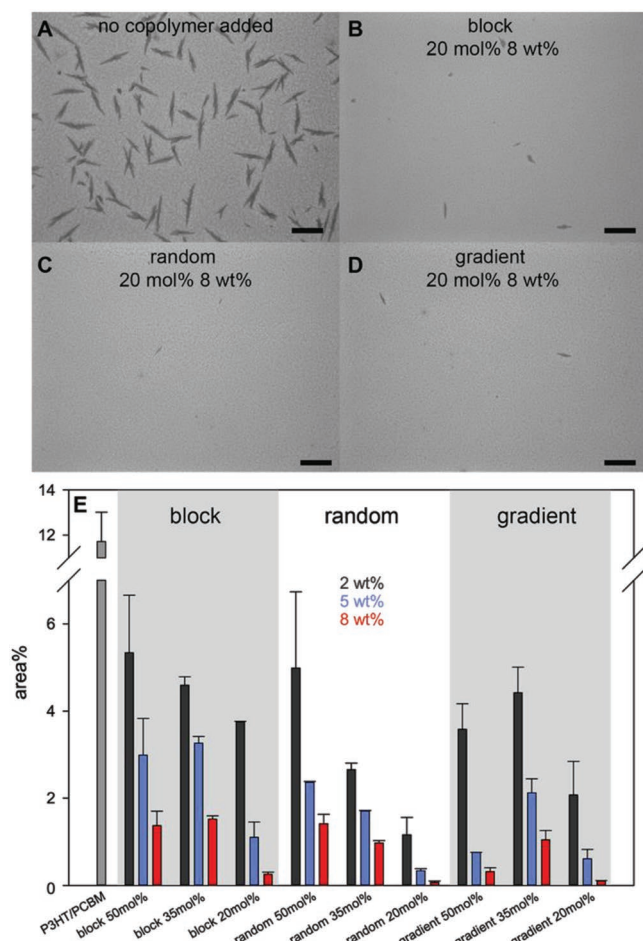
Among the 28 films examined, the random and gradient copolymers showed the least macroscale phase separation overall. Because the random copolymer with 20 mol% fullerene side chains and at 8 wt% concentration was both the best compatibilizer and the easiest to access synthetically, we focused the following device studies on this copolymer alone, comparing P3HT:PC$_{61}$BM blends with and without it.
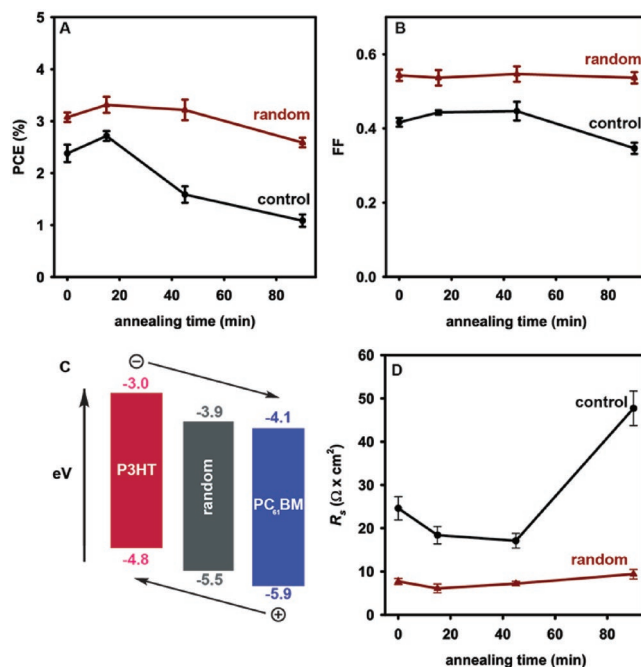
2.3. Device Performance and Longevity

The PCE depends on the efficiencies of absorption and exciton dissociation, as well as the electron and hole mobilities. Although we anticipated that the random copolymer devices would have a more stable PCE during annealing due to the copolymer's morphology-stabilizing properties, it was unclear what effect the copolymer additive would have on the other processes that contribute to PCE. To elucidate its effect, photovoltaic devices were fabricated using an inverted device architecture: glass/ITO/ZnO/polymer blend/MoO$_3$/Ag (p. S5, Supporting Information).[36] The polymer blend was prepared by spin-casting a P3HT:PC$_{61}$BM solution with or without random copolymer additive to achieve a final thickness of ≈175 nm (pp. S3 and S4, Supporting Information). Photovoltaic measurements were performed under simulated AM 1.5G conditions both before and after annealing. To obtain statistically significant results, each data point represents an average of six

Scheme 4. Postpolymerization transformation to generate random, block, and gradient copolymers with fullerene-functionalized side chains. IR spectra and GPC traces of the block copolymer (20 mol%) before and after the reaction.

Figure 2. A–D) Optical microscope images of P3HT:copolymer additive:PC$_{61}$BM blends after annealing at 150 °C for 1 h (scale bar = 30 µm). E) The relative area% of PC$_{61}$BM aggregates within each blend as a function of the copolymer sequence, composition, and concentration.

Figure 3. Plots of the A) power conversion efficiency (PCE), B) fill factor (FF), and D) series resistance (R_s) versus annealing time for P3HT:PC$_{61}$BM devices with and without random copolymer (20 mol%, 8 wt%). C) Schematic comparing the HOMO/LUMO levels of the copolymer relative to P3HT and PC$_{61}$BM.

measurements obtained from three different devices fabricated on two different substrates.

Devices containing the random copolymer additive exhibited an unexpectedly higher initial PCE ($3.1 \pm 0.2\%$) than the control device ($2.4 \pm 0.2\%$) (**Figure 3**A, Figures S56 and S57, Supporting Information). The observed PCE increase is largely attributable to a higher fill factor (FF), which is proportional to the maximum power available from a solar cell (Figure 3B). This FF difference is not due to an increase in the absorption efficiency because the copolymer has a nearly identical absorption spectrum to the P3HT:PC$_{61}$BM blend (Figure S62, Supporting Information). We hypothesized that the copolymer might instead facilitate exciton dissociation because its highest occupied molecular orbital (HOMO) and lowest unoccupied molecular orbital (LUMO) levels both lie between those of P3HT and PC$_{61}$BM, providing an "energy cascade" (Figure 3C, Figures S62 and S63, Supporting Information).[37] In addition, we observed that the electron current was significantly higher in the blends containing the random copolymer than those with none (202 ± 47 pA µm^{-2} vs 88 ± 11 pA µm^{-2}, Figure S64, Supporting Information).[38] This increased electron mobility

may be due to better charge migration away from the interface through the fullerene units in the copolymer (**Scheme 5**). To support this hypothesis, we compared the series resistances (R_s), which reflects the overall device resistance (Figure 3D). The device containing random copolymer exhibited a significantly lower series resistance, consistent with the notion that the copolymer plays an active role in exciton dissociation and electron percolation. Finally, atomic force microscope images revealed that the films containing random copolymer exhibited smaller feature sizes with larger interfacial area than the control (Figure S65, Supporting Information). More interfacial area should translate to more efficient exciton dissociation and an ensuing higher PCE. To summarize these studies, the random copolymer had an unanticipated beneficial impact on the initial device PCE by enhancing both exciton dissociation and electron percolation and mobility.

To determine device stabilities over time, thermal studies were performed by annealing the active layer at 150 °C before
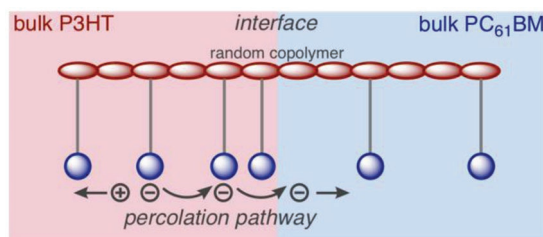
Scheme 5. Proposed percolation pathway in which electron mobility is facilitated at the interface by the side-chain fullerenes on the random copolymer.

MoO_3/Ag deposition. Devices containing random copolymer significantly outlasted and outperformed the control devices (Figure 3 and Figures S56–S59, Supporting Information). After annealing for 90 min the control device lost >50% of its initial PCE; however, the random copolymer-containing device lost just 15% of its initial PCE (Figure 3A). The biggest change in the control device was a significant drop (>50%) in the short-circuit current (J_{sc}), which reflects charge generation and collection processes (Figure S57, Supporting Information). This result can be rationalized in conjunction with the micrometer-scale phase segregation occurring during this time. These morphological changes reduce the donor/acceptor interfacial area, decreasing the exciton dissociation efficiency. This conclusion is supported by the changes in R_s,[39] which for the control device increases from 24.6 to 47.7 Ω cm^2 after annealing (Figure 3D). Combined, these data suggest that by stabilizing the active layer morphology, the random copolymer compatibilizer also stabilizes the device PCE.

Although the random copolymer led to a longer-lasting device, a minor but significant drop in PCE was observed. The culprit was a decrease in open-circuit voltage (V_{oc}, Figure S57, Supporting Information), which reflects the amount of charge recombination. Further analysis showed that the reverse bias saturation current (J_0),[40] which also reflects the amount of charge recombination, was one order of magnitude higher with random copolymer present (Figure S61, Supporting Information). The theoretical V_{oc} change expected from this J_0 difference is ≈ 0.07 V, consistent with the experimental differences in V_{oc} (p. S65, Supporting Information). Combined, the V_{oc} drop and increased J_0 imply that after annealing the copolymer additive facilitates some charge recombination.

3. Conclusions

While PCEs have been on the rise for organic photovoltaics, the poor longevity of these devices remains a concern. We demonstrated that a random copolymer additive can both enhance longevity and improve efficiency. Other areas for future exploration include understanding the increased charge recombination that occurs after annealing as well as how the transport layer interfaces are affected by compatibilizer. Overall, this approach to stabilize organic photovoltaics should be generalizable, and our future efforts are focused on applying it toward higher efficiency conjugated polymer-based devices.

Supporting Information

Supporting Information is available from the Wiley Online Library or from the author.

Conflict of Interest

The authors declare no conflict of interest.

[1] National Renewable Energy Lab, Best Research-Cell Efficiencies, https://www.nrel.gov/pv/assets/images/efficiency-chart.png (accessed: June 2018).

[2] For recent reviews, see: a) G. Zhang, J. Zhao, P. C. Y. Chow, K. Jiang, J. Zhang, Z. Zhu, J. Zhang, F. Huang, H. Yan, *Chem. Rev.* **2018**, *118*, 3447; b) J. Hou, O. Inganäs, R. H. Friend, F. Gao, *Nat. Mater.* **2018**, *17*, 119; c) S. Holliday, Y. Li, C. K. Luscombe, *Prog. Polym. Sci.* **2017**, *70*, 34; d) H. Huang, L. Yang, B. Sharma, *J. Mater. Chem. A* **2017**, *5*, 11501; e) Y. Gao, M. Liu, Y. Zhang, Z. Liu, Y. Yang, L. Zhao, *Polymers* **2017**, *9*, 39; f) Z. Hu, L. Ying, F. Huang, Y. Cao, *Sci. China: Chem.* **2017**, *60*, 571; g) S. Xiao, Q. Zhang, W. You, *Adv. Mater.* **2017**, *29*, 1601391; h) L. Ying, F. Huang, G. C. Bazan, *Nat. Commun.* **2017**, *8*, 14047.

[3] a) F. C. Krebs, N. Espinosa, M. Hösel, R. R. Søndergaard, M. Jørgensen, *Adv. Mater.* **2014**, *26*, 29; b) R. R. Søndergaard, M. Hösel, F. C. Krebs, *J. Polym. Sci., Part B: Polym. Phys.* **2013**, *51*, 16; c) R. Søndergaard, M. Hösel, D. Angmo, T. T. Larsen-Olsen, F. C. Krebs, *Mater. Today* **2012**, *15*, 36.

[4] For reviews and recent examples of fullerene-free devices, see: a) S. Li, L. Ye, W. Zhao, H. Yan, B. Yang, D. Liu, W. Li, H. Ade, J. Hou, *J. Am. Chem. Soc.* **2018**, *140*, 7159; b) Z. Fei, F. D. Eisner, X. Jiao, M. Azzouzi, J. A. Röhr, Y. Han, M. Shahid, A. S. R. Chesman, C. D. Easton, C. R. McNeill, T. D. Anthopoulos, J. Nelson, M. Heeney, *Adv. Mater.* **2018**, *30*, 1705209; c) P. Cheng, G. Li, X. Zhan, Y. Yang, *Nat. Photonics* **2018**, *12*, 131; d) X. Xu, T. Yu, Z. Bi, W. Ma, Y. Li, Q. Peng, *Adv. Mater.* **2018**, *30*, 1703973; e) W. Zhao, S. Li, H. Yao, S. Zhang, Y. Zhang, B. Yang, J. Hou, *J. Am. Chem. Soc.* **2017**, *139*, 7148; f) W. Chen, Q. Zhang, *J. Mater. Chem. C* **2017**, *5*, 1275.

[5] For reviews and examples of fullerene-containing devices, see: a) J. Zhao, S. Zhao, Z. Xu, D. Song, B. Qiao, D. Huang, Y. Zhu, Y. Li, Z. Li, Z. Qin, *ACS Appl. Mater. Interfaces* **2018**, *10*, 24075; b) C. Xu, M. Wright, N. K. Elumalai, M. A. Mahmud, D. Wang, V. R. Goncales, M. B. Upama, F. Haque, J. J. Gooding, A. Uddin, *Appl. Phys. A* **2018**, *124*, 449; c) Y. Liu, M. Sheri, M. D. Cole, T. Emrick, T. P. Russell, *Angew. Chem., Int. Ed.* **2018**, *57*, 9675; d) J. Zhang, R. Xue, G. Xu, W. Chen, G.-Q. Bian, C. Wei, Y. Li, Y. Li, *Adv. Funct. Mater.* **2018**, *28*, 1705847; e) X. Liu, L. Nian, K. Gao, L. Zhang, L. Qing, Z. Wang, L. Ying, Z. Xie, Y. Ma, Y. Cao, F. Liu, J. Chen, *J. Mater. Chem. A* **2017**, *5*, 17619; f) C. Li, H. Zhu, Y. Wang, H. Liu, S. Hu, F. Wang, B. Zhang, S. Dai, Z. Tan, *Nano Energy* **2017**, *31*, 201; g) J. Huang, J. H. Carpenter, C.-Z. Li, J.-S. Yu, H. Ade, A. K.-Y. Jen, *Adv. Mater.* **2016**, *28*, 967; h) J. Zhao, Y. Li, G. Yang, K. Jiang, H. Lin, H. Ade, W. Ma, H. Yan, *Nat. Energy* **2016**, *1*, 15027.

[6] K. Bourzac, *C&EN Global Enterp.* **2018**, *96*, 7.

[7] For reviews on stability (including, but not limited to, morphological stability), see: a) S. Rafique, S. M. Abdullah, K. Sulaiman,

M. Iwamoto, *Renewable Sustainable Energy Rev.* **2018**, *84*, 43; b) S. A. Gevorgyan, I. M. Heckler, E. Bundgaard, M. Corazza, M. Hösel, R. R. Søndergaard, G. A. dos Reis Benatto, M. Jørgensen, F. C. Krebs, *J. Phys. D: Appl. Phys.* **2017**, *50*, 103001; c) W. R. Mateker, M. D. McGehee, *Adv. Mater.* **2017**, *29*, 1603940; d) P. Cheng, X. Zhan, *Chem. Soc. Rev.* **2016**, *45*, 2544; e) S. Lizin, S. Van Passel, E. De Schepper, W. Maes, L. Lutsen, J. Manca, D. Vanderzande, *Energy Environ. Sci.* **2013**, *6*, 3136; f) M. Jørgensen, K. Norrman, S. A. Gevorgyan, T. Tromholt, B. Andreasen, F. C. Krebs, *Adv. Mater.* **2012**, *24*, 580.

[8] a) B. Kuei, E. D. Gomez, *Soft Matter* **2017**, *13*, 49; b) F. S. Bates, *Science* **1991**, *251*, 898.

[9] For recent reviews, see: a) P. Cheng, X. Zhan, *Mater. Horiz.* **2015**, *2*, 462; b) F. Goubard, G. Wantz, *Polym. Int.* **2014**, *63*, 1362.

[10] For recent examples, see: a) M. Xiao, K. Zhang, Y. Jin, Q. Yin, W. Zhong, F. Huang, Y. Cao, *Nano Energy* **2018**, *48*, 53; b) G. Sai-Anand, A. Dubey, A.-I. Gopalan, S. Venkatesan, S. Ruban, K. M. Reza, J. Choi, K. S. Lakhi, B. Xu, Q. Qiao, A. Vinu, *Sol. Energy Mater. Sol. Cells* **2018**, *182*, 246; c) A. Rahmanudin, X. A. Jeanbourquin, S. Hänni, A. Sekar, E. Ripaud, L. Yaoa, K. Sivula, *J. Mater. Chem. A* **2017**, *5*, 17517; d) H. Li, K. Lu, Z. Wei, *Adv. Energy Mater.* **2017**, *7*, 1602540; e) P. Cheng, C. Yan, T-K. Lau, J. Mai, X. Lu, X. Zhan, *Adv. Mater.* **2016**, *28*, 5822; f) P. Cheng, Q. Shi, X. Zhan, *Acta Chim. Sin.* **2015**, *73*, 252; g) W. Zhou, J. Shi, L. Lv, L. Chen, Y. Chen, *Phys. Chem. Chem. Phys.* **2015**, *17*, 387; h) J. Yang, W. He, K. Denman, Y. Jiang, Y. Qin, *J. Mater. Chem. A* **2015**, *3*, 2108; i) Q. An, F. Zhang, L. Li, J. Wang, Q. Sun, J. Zhang, W. Tang, Z. Deng, *ACS Appl. Mater. Interfaces* **2015**, *7*, 3691; j) W. Nie, G. Gupta, B. K. Crone, F. Liu, D. L. Smith, P. P. Ruden, C.-Y. Kuo, H. Tsai, H.-L. Wang, H. Li, S. Tretiak, A. D. Mohite, *Adv. Sci.* **2015**, *2*, 1500024; k) S. Wang, Y. Qu, S. Li, F. Ye, Z. Chen, X. Yang, *Adv. Funct. Mater.* **2015**, *25*, 748.

[11] For recent reviews, see: a) D. Kipp, R. Verduzco, V. Ganesan, *Mol. Syst. Des. Eng.* **2016**, *1*, 353; b) K. Yuan, L. Chen, Y. Chen, *Polym. Int.* **2014**, *63*, 593; c) See also, ref. [9a].

[12] For recent examples, see: a) C. Sartorio, V. Campisciano, C. Chiappara, S. Cataldo, M. Scopelliti, M. Gruttadauria, F. Giacalone, B. Pignataro, *J. Mater. Chem. A* **2018**, *6*, 3884; b) Y. Sun, P. Pitliya, C. Liu, X. Gong, D. Raghavan, A. Karim, *Polymer* **2017**, *113*, 135; c) D. Kipp, O. Wodo, B. Ganapathysubramanian, V. Ganesan, *Sol. Energy Mater. Sol. Cells* **2017**, *161*, 206; d) F. Lombeck, A. Sepe, R. Thomann, R. H. Friend, M. Sommer, *ACS Nano* **2016**, *10*, 8087; e) H. Fujita, T. Michinobu, S. Fukuta, T. Koganezawa, T. Higashihara, *ACS Appl. Mater. Interfaces* **2016**, *8*, 5484; f) S. Kakogianni, A. K. Andreopoulou, J. K. Kallitsis, *Polymers* **2016**, *8*, 440; g) D. Kipp, V. Ganesan, *Macromolecules* **2016**, *49*, 5137; h) S. Kakogianni, M. A. Lebedeva, G. Paloumbis, A. K. Andreopoulou, K. Porfyrakis, J. K. Kallitsis, *RSC Adv.* **2016**, *6*, 98306; i) J. W. Mok, D. Kipp, L. R. Hasbun, A. Dolocan, J. Strzalka, V. Ganesan, R. Verduzco, *J. Mater. Chem. A* **2016**, *4*, 14804; j) J. Liu, X. Zhu, J. Li, J. Shen, G. Tu, *RSC Adv.* **2016**, *6*, 61934; k) K. H. Park, Y. An, S. Jung, H. Park, C. Yang, *Energy Environ. Sci.* **2016**, *9*, 3464; l) E. Bicciocchi, M. Haeussler, E. Rizzardo, A. D. Scully, K. P. Ghiggino, *J. Polym. Sci., Part A: Polym. Chem.* **2015**, *53*, 888; m) M. Raïssi, H. Erothu, E. Ibarboure, H. Cramail, L. Vignau, E. Cloutet, R. C. Hiorns, *J. Mater. Chem. A* **2015**, *3*, 18207; n) D. Kipp, J. Mok, J. Strzalka, S. B. Darling, V. Ganesan, R. Verduzco, *ACS Macro Lett.* **2015**, *4*, 867.

[13] A. Li, J. Amonoo, B. Huang, P. K. Goldberg, A. J. McNeil, P. F. Green, *Adv. Funct. Mater.* **2014**, *24*, 5594.

[14] a) J. A. Amonoo, A. Li, G. E. Purdum, M. E. Sykes, B. Huang, E. F. Palermo, A. J. McNeil, M. Shtein, Y.-L. Loo, P. F. Green, *J. Mater. Chem. A* **2015**, *3*, 20174; b) E. F. Palermo, A. J. McNeil,

in *Sequence-Controlled Polymers: Synthesis, Self-Assembly, and Properties*, ACS Symposium Series, Vol. *1170* (Eds: H. Baltes, W. Göpel, J. Hesse), American Chemical Society, Washington, DC **2014**, Ch. 19; c) E. F. Palermo, H. L. van der Laan, A. J. McNeil, *Polym. Chem.* **2013**, *4*, 4606; d) E. F. Palermo, A. J. McNeil, *Macromolecules* **2012**, *45*, 5948; e) J. R. Locke, A. J. McNeil, *Macromolecules* **2010**, *43*, 8709.

[15] E. F. Palermo, S. B. Darling, A. J. McNeil, *J. Mater. Chem. C* **2014**, *2*, 3401.

[16] For recent reviews, see: a) M. A. Baker, C.-H. Tsai, K. J. T. Noonan, *Chem. - Eur. J.* **2018**, *24*, 13078; b) A. K. Leone, A. J. McNeil, *Acc. Chem. Res.* **2016**, *49*, 2822; c) T. Yokozawa, Y. Ohta, *Chem. Rev.* **2016**, *116*, 1950; d) R. Grisorio, G. P. Suranna, *Polym. Chem.* **2015**, *6*, 7781; e) Z. J. Bryan, A. J. McNeil, *Macromolecules* **2013**, *46*, 8395.

[17] a) H. A. Brontstein, C. K. Luscombe, *J. Am. Chem. Soc.* **2009**, *131*, 12894; b) N. Doubina, A. Ho, A. K.-Y. Jen, C. K. Luscombe, *Macromolecules* **2009**, *42*, 7670; c) V. Senkovskyy, R. Tkachov, T. Beryozkina, H. Komber, U. Oertel, M. Horecha, V. Bocharova, M. Stamm, S. A. Gevorgyan, F. C. Krebs, A. Kiriy, *J. Am. Chem. Soc.* **2009**, *131*, 16445; d) V. Senkovskyy, M. Sommer, R. Tkachov, H. Komber, W. T. S. Huck, A. Kiriy, *Macromolecules* **2010**, *43*, 10157.

[18] See also: a) A. O. Hall, S. R. Lee, A. N. Bootsma, J. W. G. Bloom, S. E. Wheeler, A. J. McNeil, *J. Polym. Sci., Part A: Polym. Chem.* **2017**, *55*, 1530; b) S. R. Lee, J. W. G. Bloom, S. E. Wheeler, A. J. McNeil, *Dalton Trans.* **2013**, *42*, 4218; c) E. L. Lanni, A. J. McNeil, *J. Am. Chem. Soc.* **2009**, *131*, 16573.

[19] For a related structure, see: S. H. Chan, C. S. Lai, H. L. Chen, C. Ting, C. P. Chen, *Macromolecules* **2011**, *44*, 8886.

[20] All copolymerizations presented in Figure 1 were conducted under N (outside the glovebox) at 0 °C so that the slower reaction rate would enable adequate time between aliquots.

[21] M. Wong, J. Hollinger, L. M. Kozycz, T. M. McCormick, Y. Lu, D. C. Burns, D. S. Seferos, *ACS Macro Lett.* **2012**, *1*, 1266.

[22] See also: L. Zhai, R. L. Pilston, K. L. Zaiger, K. K. Stokes, R. D. McCullough, *Macromolecules* **2003**, *36*, 61.

[23] For a recent review, see: C. J. Pickens, S. N. Johnson, M. M. Pressnall, M. A. Leon, C. J. Berkland, *Bioconjugate Chem.* **2018**, *29*, 686.

[24] S.-H. Chan, C.-S. Lai, H.-L. Chen, C. Ting, C.-P. Chen, *Macromolecules* **2011**, *44*, 8886.

[25] M. Li, P. Xu, J. Yang, S. Yang, *J. Mater. Chem.* **2010**, *20*, 3953.

[26] a) F. Pierini, M. Lanzi, P. Nakielski, S. Pawlowska, O. Urbanek, K. Zembrzcyki, T. A. Kowalewski, *Macromolecules* **2017**, *50*, 4972; b) M. Lanzi, E. Salatelli, T. Benelli, D. Caretti, L. Giorgini, F. P. Di-Nicola, *J. Appl. Polym. Sci.* **2015**, *132*, 42121.

[27] M. Chen, M. Li, H. Wang, S. Qu, X. Zhao, L. Xie, S. Yang, *Polym. Chem.* **2013**, *4*, 550.

[28] B. Yameen, T. Puerchkhauer, J. Ludwig, I. Ahmed, O. Altintas, L. Fruk, A. Colsmann, C. Barner-Kowollik, *Small* **2014**, *10*, 3091.

[29] N. E. Mbua, J. Guo, M. A. Wolfert, R. Steet, G.-J. Boons, *ChemBioChem* **2011**, *12*, 1912.

[30] S. P. Singh, C. P. Kumar, G. D. Sharma, R. Kurchania, M. S. Roy, *Adv. Funct. Mater.* **2012**, *22*, 4087.

[31] S. Wang, X. Yang, W. Zhu, L. Zou, K. Zhang, Y. Chen, F. Xi, *Polymer* **2014**, *55*, 4812.

[32] Copolymers with >50 mol% side-chain fullerenes were largely insoluble in THF and not pursued further.

[33] An exothermic peak was observed at temperatures >150 °C during DSC analysis of some fullerene-functionalized copolymers (Figures S66 and S67, Supporting Information). After DSC analysis, the samples were completely insoluble in CDCl$_3$. We tentatively

attributed this nonreversible event to a crosslinking reaction involving side-chain azides (<5% by IR spectroscopy) reacting with fullerene. Fortunately, this reaction does not occur if the copolymer samples are heated to the device annealing temperature (150 °C). After DSC analysis, the resulting copolymers fully dissolve in CDCl$_3$ and the ^{1}H NMR spectra are identical to the samples before analysis (Figure S67, Supporting Information).

[34] A. Torreggiani, F. Tinti, A. Savoini, M. Melchiorre, R. Po, N. Camaioni, *Org. Photonics Photovoltaics* **2014**, *2*, 50.

[35] a) J. Zhao, A. Swinnen, G. Van Assche, J. Manca, D. Vanderzande, B. Van Mele, *J. Phys. Chem. B* **2009**, *113*, 1587; b) P. E. Hopkinson, P. A. Staniec, A. J. Pearson, A. D. F. Dunbar, T. Wang, A. J. Ryan, R. A. L. Jones, D. G. Lidzey, A. M. Donald, *Macromolecules* **2011**, *44*, 2908; c) H. Chen, J. Chen, W. Yin, X. Yu, M. Shao, K. Xiao, K. Hong, D. L. Pickel, W. M. Kochemba, S. M. KilbeyII, M. Dadmun, *J. Mater. Chem. A* **2013**, *1*, 5309.

[36] Z. He, C. Zhong, S. Su, M. Xu, H. Wu, Y. Cao, *Nat. Photonics* **2012**, *6*, 591.

[37] a) J. Hou, Z. Tan, Y. Yan, Y. He, C. Yang, Y. Li, *J. Am. Chem. Soc.* **2006**, *128*, 4911; b) Y. He, G. Zhao, B. Peng, Y. Li, *Adv. Funct. Mater.* **2010**, *20*, 3383.

[38] Note that blends containing 12 wt% random copolymer exhibited lower electron mobilities than the 8 wt% blend, and lower hole mobilities than the control devices, suggesting there is an upper limit to additive concentration on its beneficial effects (Figures S56 and S57, Supporting Information). We suspect that at these higher concentrations the copolymer may disrupt the P3HT crystallization within its "pure" domain.

[39] M.-S. Kim, B.-G. Kim, J. Kim, *ACS Appl. Mater. Interfaces* **2009**, *1*, 1264.

[40] a) J. D. Zimmerman, X. Xiao, C. K. Renshaw, S. Wang, V. V. Diev, M. E. Thompson, S. R. Forrest, *Nano Lett.* **2012**, *12*, 4366; b) W. J. Potscavage Jr., A. Sharma, B. Kippelen, *Acc. Chem. Res.* **2009**, *42*, 1758; c) C. G. Shuttle, A. Maurano, R. Hamilton, B. O'Regan, J. C. de Mello, J. R. Durrant, *Appl. Phys. Lett.* **2008**, *93*, 183501.